Energy spectrum and structure of thin pseudomorphic InAs quantum wells in an AlAs matrix: Photoluminescence spectra and band-structure calculations

Timur S. Shamirzaev,* Alexanser M. Gilinsky, Alexanser K. Kalagin, Alexey V. Nenashev, and Konstantin S. Zhuravlev
Institute of Semiconductor Physics, Prospekt Lavrentieva, 13, Novosibirsk 630090, Russia
(Received 12 May 2007; revised manuscript received 6 August 2007; published 11 October 2007)

The energy spectrum of thin pseudomorphic InAs quantum wells (QWs) in an AlAs matrix has been studied by steady-state and transient photoluminescence (PL) and calculation. It has been found that the PL spectra of the QWs consist of intense lines related to a no-phonon excitonic transition accompanied by its phonon replicas. The band alignment in the QWs is shown to be of type I, with the lowest conduction band states belonging to the indirect X_{XY} minimum.

DOI: 10.1103/PhysRevB.76.155309 PACS number(s): 73.21.Fg, 78.67.De, 78.55.Cr, 73.20.At

I. INTRODUCTION

Thin InAs and InGaAs quantum wells (QWs) recently have attracted much attention from both the fundamental and application points of view.[1–16] The majority of the studies reported so far have concentrated on the direct gap InGaAs/GaAs material system,[1–4,6,7,12,13] while the technologically similar system of InAs/AlAs received much less attention. Usually, a QW of the InGaAs/AlAs system is considered to be similar to InAs/GaAs QWs. There, however, exist important differences in the physical properties between InGaAs/GaAs and InGaAs/AlAs QWs which have not been addressed so far. The principal difference between the InAs QWs in GaAs and AlAs concerns the band structure of the QWs that could switch from direct to indirect gap due to the changes in the relative positions of various conduction band minima. Because of the small electron effective mass of InAs, the electron states in the Γ minimum of the QW conduction band are considerably more strongly shifted by quantum confinement than those in the L and X minima. Therefore, in the InGaAs/AlAs material system, the confinement can lead to a transformation of the structure of electronic levels in the QW due to (i) a transition of the lowest state of the conduction band from direct to indirect, and (ii) a transition of the band alignment from type I to type II, which can happen if quantum confinement pushes the lowest state of the QW conduction band above that of the matrix.

For thin InGaAs/AlAs QWs with a small InAs mole fraction, the type-I to type-II transition was experimentally demonstrated by many groups.[14–16] However, in spite of many experimental and theoretical investigations devoted to the study of the structure of electronic levels of thin InAs layers,[2–13] only the conduction band states of the Γ minimum were taken into consideration to date. At the same time, the effect of the confinement on the structure of electronic levels of thin InAs QWs has been scarcely studied yet.

In this paper, we present the results of a study of atomic structure and energy spectrum of single thin InAs QWs in an AlAs matrix. We demonstrate that the quantum confinement leads to the transformation of the lowest electron state from the direct Γ to indirect X minimum of the InAs conduction band, but does not result in a type-I to type-II transition of spatial band alignment.

The paper is organized as follows. In Sec. II, we demonstrate that the lack of precise knowledge on the InAs/AlAs QW atomic structure and uncertainties of some of the band-structure parameters of InAs hinder the unambiguous calculation of the QW band lineup. In Sec. III, the techniques used for experimental assessment of the band structure are described. The experimental results on continuous-wave (cw) and transient photoluminescence (PL) of the QWs are presented in Sec. IV together with a discussion of the shape of the QW PL spectrum and PL decay. The analysis of the experimental dependence of the QW PL line position on carrier concentration and a comparison of the positions of the PL lines with the calculated transition energies allow us to clarify the band lineup and atomic structure of the QWs. Finally, the conclusions are summarized in Sec. V.

II. CALCULATION OF THE BAND LINEUP OF A THIN InAs/AlAs QUANTUM WELL

In this section, we will demonstrate that, despite the expectation, the available literature data are insufficient for the calculation of the band structure of a thin InAs quantum well in a wide band-gap matrix with adequate accuracy.

Traditionally, thin InAs QWs have been described as thin slabs with abrupt heterointerfaces[2–10] (we will refer to such QWs as abrupt). However, Offermans *et al.*[13] recently demonstrated a strong intermixing of the well and barrier materials in thin InAs QWs in both GaAs and AlAs matrices due to the strain-driven InAs segregation (such QWs will be referred to as diffused in the following). In this section, we present a band lineup calculation for both the abrupt and diffused QWs. In order to calculate the band lineup of a strained InAs/AlAs heterostructure, we take into account (i) the change of the band gaps of InAs and AlAs due to the change in the unit cell volume ($\Delta\Omega/\Omega$), (ii) the splitting of the degenerate valence bands and of the degenerate indirect minima in the conduction band of InAs and AlAs induced by the biaxial component (I) of the strain, and (iii) the value of the InAs/AlAs valence band offset (VBO).[17]

A. Case of a thin abrupt quantum well

If a thin InAs/AlAs QW manifests itself as a thin slab as was supposed earlier for InAs/GaAs and InAs/InP QWs,[2–10] the strain is mostly localized within the InAs layer, and therefore, the change of the band gaps and the splitting of the

degenerate bands can be easily calculated using the macroscopic theory of elasticity.[17,18] For a pseudomorphic InAs layer, the components of the strain tensor parallel $\epsilon_{\parallel}$ and perpendicular $\epsilon_{\perp}$ to the plane of the heterointerface are given by[17]

$$\epsilon_{\parallel} = \frac{a_{\parallel}}{a_{\mathrm{InAs}}} - 1, \tag{1}$$

$$\epsilon_{\perp} = \frac{a_{\perp}}{a_{\mathrm{InAs}}} - 1, \tag{2}$$

$$a_{\perp} = a_{\mathrm{InAs}}\left[1 - 2\epsilon_{\parallel}\frac{c_{12}}{c_{11}}\right], \tag{3}$$

where $a_{\parallel}$ and $a_{\perp}$ are the lattice parameters of the strained InAs in the plane and perpendicular to the layer, respectively, with $a_{\parallel}$ equal to the cubic lattice parameter of the AlAs, a_{InAs} is the lattice parameter of unstrained InAs, and c_{12} and c_{11} are the elastic constants of InAs. Let us choose the Cartesian coordinate system with the z axis oriented along the sample growth direction. Then the components of the strain tensor will be $\epsilon_{xx}=\epsilon_{yy}=\epsilon_{\parallel}$ and $\epsilon_{zz}=\epsilon_{\perp}$, the change of the unit cell volume due to the hydrostatic part of the strain can be written as $\Delta\Omega/\Omega=\mathrm{Tr}(\epsilon)=\epsilon_{xx}+\epsilon_{yy}+\epsilon_{zz}$, and the biaxial component of the strain will be $I=\epsilon_{zz}-\epsilon_{xx}$.

According to Ref. 19, the changes of the band gaps for direct and indirect extrema with unit cell volume are given by $E_g=E_g^0+a_v\Delta\Omega/\Omega$, where E_g^0 is the unstrained band gap and a_v is the absolute deformation potential that describes the change of the total band gap. The twofold degenerate valence band of unstrained InAs splits into separate heavy- (HH) and light-hole (LH) bands. Taking into account the biaxial component of the strain and spin-orbit coupling, the splitting of the valence bands (ΔE_{HH-LH}) can be expressed using the components of the strain tensor, the deformation potential b, and the spin-orbit splitting:[17]

$$\Delta E_{HH-LH} = \frac{\Delta_0}{2} - \frac{3\delta E_{001}}{4} - \frac{1}{2}\left(\Delta_0{}^2 + \frac{1}{2}\Delta_0\delta E_{001} + \frac{4}{9}\delta E_{001}^2\right)^{1/2}, \tag{4}$$

where Δ_0 is the spin-orbit splitting in the absence of strain and $\delta E_{001}=2bI$ is the splitting due to biaxial strain. In unstrained bulk InAs, the X minimum of the conduction band is anisotropic, with the X_X, X_Y, and X_Z states being threefold degenerate. The biaxial compression of a thin InAs layer grown on AlAs results in lowering the energy of the X_X and X_Y states with respect to that of the X_Z state.[20] Thus, the lowest state of the X minimum in an InAs/AlAs structure becomes the twofold degenerate X_{XY} state. The shifts of the states with respect to the unperturbed X minimum position are given for the X_{XY} and X_Z states by the expressions[20]

$$\Delta E_Z = \frac{2E_2I}{3} \tag{5}$$

and

TABLE I. Band-structure parameters for InAs and AlAs.

Parameters	InAs	AlAs
a (Å)	6,0583[a]	5.6611[a]
c_{11} (Mbar)	0.833[a]	1.250[a]
c_{12} (Mbar)	0.453[a]	0.534[a]
b (eV)	−1.8[a,b]	−2.3[b]
Δ_0 (eV)	0.38[a,b]	0.28[a,b]
E_2 (eV)	3.7[c]	6.11[c]
a_v^{Γ} (eV)	−5.66[d]	−8.93[d]
a_v^{X} (eV)	0.92[d]	1.01[d]
a_v^{L} (eV)	−2.89[d]	−4.60[d]
E_{Γ} (eV)	0.417[b]	3.099[b]
E_X (eV)	1.39,[e] 1.433,[b] 2.27[f,g]	2.228,[h] 2.24[b]
E_L (eV)	0.98,[e] 1.133,[b] 1.52[f,g]	2.46[b]

[a]Reference 17.
[b]Reference 21.
[c]Reference 20.
[d]Reference 19.
[e]Reference 22.
[f]Reference 24.
[g]Reference 25.
[h]Reference 23.

$$\Delta E_{XY} = -\frac{E_2I}{3}, \tag{6}$$

where E_2 is the deformation potential at point X of the Brillouin zone.[20] The L minimum of the conduction band is also anisotropic and threefold degenerate, however, (001) biaxial strain has negligible effect on this minimum.[17]

In order to calculate the band lineup of a thin pseudomorphic InAs/AlAs QW, we used the band-structure parameters of InAs and AlAs collected in Table I.

Unfortunately, together with accurately experimentally determined or calculated parameters such as lattice constants, elastic constants, spin-orbit splitting, and deformation potentials, there are parameters with poorly known values. Actually, the low temperature energy gaps for the X (E_X) and L (E_L) conduction band minima in InAs have not been studied experimentally. Vurgaftman *et al.*[21] recommended using $E_X=1.433$ eV and $E_L=1.133$ eV based on the suggestions made by Adachi,[26] and Ref. 27 extrapolated E_X and E_L from room temperature data to 0 K, taking the temperature dependence of the indirect gaps to be identical to that of the direct gap. On the other hand, Ref. 22 gives $E_X=1.39$ eV and $E_L=0.98$ eV, while Boykin[24] and Ref. 25 give $E_X=2.27$ eV and $E_L=1.152$ eV, respectively. The VBO value for the InAs/AlAs heterojunction is also not completely determined yet. There are many calculations for strained InAs layers on unstrained AlAs substrates which give various values of VBO ranging from 0.29 to 0.83 eV.[8,18,21,28–31]

Using the accurately determined parameters, one can calculate the following values for a pseudomorphic strained InAs layer: the direct band gap $E_{\Gamma}=0.55$ eV, the splitting between the light- and heavy-hole levels $\Delta E_{HH-LH}=0.205$ eV, and the shifts of the X_{XY} and X_Z states of the InAs conduction band with respect to their unperturbed position $\Delta E_Z=0.34$ eV and $\Delta E_{XY}=-0.17$ eV. On the other hand, the values for the unperturbed positions of the indirect

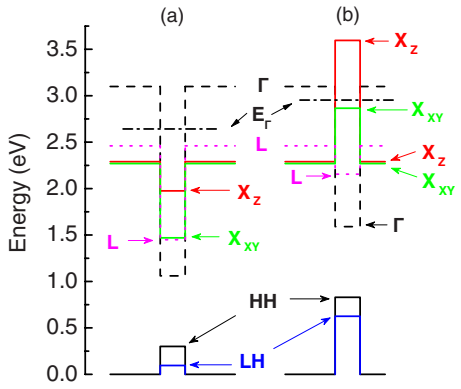

FIG. 1. (Color online) Band diagrams of pseudomorphic abrupt InAs/AlAs structure calculated with utmost values of VBO, E_X, and E_L of the InAs layer. (a) E_X=1.335 eV, E_L=1.153 eV, and VBO=0.3 eV; (b) E_X=2.215 eV, E_L=1.325 eV, and VBO =0.83 eV. E_Γ marks energy positions of the Γ-minimum electrons for an InAs QW with a thickness of 1.5 ML.

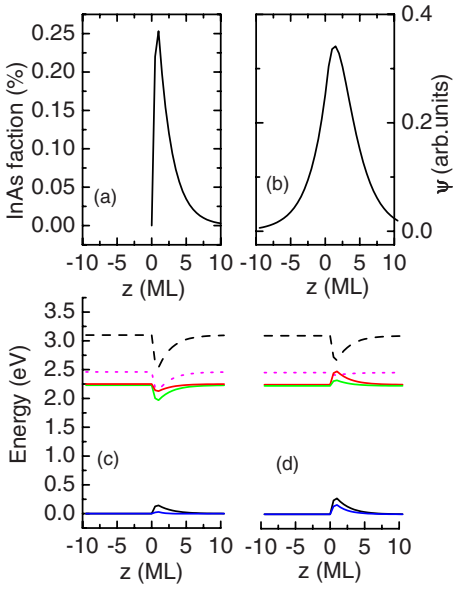

FIG. 2. (Color online) (a) The segregation profile of a diffused InAs/AlAs QW with a nominal amount of deposited InAs N=1.4 ML, calculated according to Ref. 32. (b) Wave function amplitude of an X_{XY} electron in the diffused QW with type-I band structure. [(c) and (d)] The band lineups of the diffused QWs for two utmost sets of values of E_X, E_L, and VBO determined by a linear approximation between the parameters of InAs and AlAs. From top to bottom: Γ, L, X_Z, and X_{XY} conduction band minima, and HH and LH valence bands.

extrema that are calculated from less precisely known parameters vary in the ranges of 1.335–2.215 eV and 1.153–1.325 eV for E_X and E_L, respectively. If we now take the utmost values of E_X, E_L, and VBO, then different band diagrams are realized as shown in Fig. 1.

Both sets of values in Fig. 1 result in a type-I alignment, with the conduction band states belonging to the Γ minimum. However, the quantum confinement in a thin InAs QW with thickness of a few monolayers leads to a strong increase in the energy of the Γ point electrons with respect to their indirect counterparts due to the small value of the electron effective mass in the Γ minimum, as is shown in Fig. 1. Therefore, if a QW manifests itself as a thin slab, both the type-I band alignment with the lowest electron state belonging to an indirect minimum of the InAs conduction band and type-II alignment can be realized depending on the values of E_X, E_L, and VBO.

B. Case of a diffused InAs quantum well

In order to describe a diffused QW, we follow Offermans *et al.*[13] and use the phenomenological model of Muraki *et al.*[32] In the framework of this model, the indium composition profile across the QW is determined by the amount of deposited InAs (N) and the segregation coefficient R that equals 0.78 for InAs in AlAs.[13] The calculated segregation profile of a QW with N=1.4 monolayers (ML) is shown in Fig. 2(a). One can see that the peak InAs fraction in the diffused layer is only 25%. The band lineup of this diffused QW was calculated using the theory of elasticity.[17,18] The band-structure parameters for the layers of InAlAs alloy were determined by a linear approximation between the parameters of InAs and AlAs. The calculated band diagrams for the two utmost cases of E_X, E_L, and VBO are depicted in Figs. 2(c) and 2(d). One can see that, similar to the case of an abrupt QW, both the type-I and type-II band alignments can be realized depending on the band parameters. However, the InAlAs alloy contains a high concentration (≥75%) of AlAs with well-defined band-structure parameters that results in a considerable decrease of the uncertainty in the E_X, E_L, and VBO values. Therefore, in the case of the diffused QW, the lowest electron state always belongs to the X_{XY} minimum of the QW conduction band.

Thus, we see that the uncertainty in the QW atomic structure and the values of E_X and E_L of InAs and VBO hamper the determination of the lineup of thin InAs/AlAs structures merely by calculation. In order to clarify the actual structure of the QW band lineup, we have performed PL experiments as described in the next sections.

III. EXPERIMENT

The samples of InAs QWs studied in this work were grown by molecular beam epitaxy on semi-insulating (001)-oriented GaAs substrates in a Riber-32P system. The samples consisted of one InAs layer sandwiched between two 25 nm thick layers of AlAs grown on top of a 200 nm buffer GaAs layer. The first AlAs layer in all the samples was grown at a substrate temperature T_S of 600 °C. The QW layers were deposited with a nominal amount of InAs of 1.2 or 1.4 ML at T_S=480 °C and a rate of 0.04 ML s^{-1}, as calibrated in the center of the wafer using reference samples. To prevent InAs evaporation, the growth temperature was not increased during the deposition of a few initial monolayers of the second AlAs layer covering the QW. The rest of the cover layer was grown at T_S=600 °C. A 20 nm GaAs cap layer was grown on top of the sandwich in order to prevent oxidation of AlAs. For comparison, three types of structures were used: (i) a

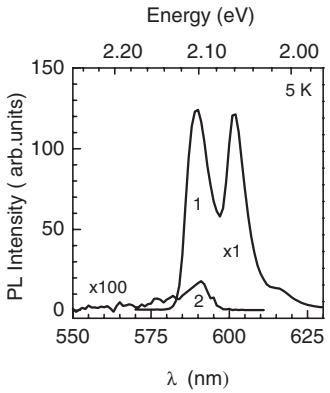

FIG. 3. The low temperature PL spectra of (1) the InAs/AlAs QW with 1.4 ML thickness and (2) the AlAs layer.

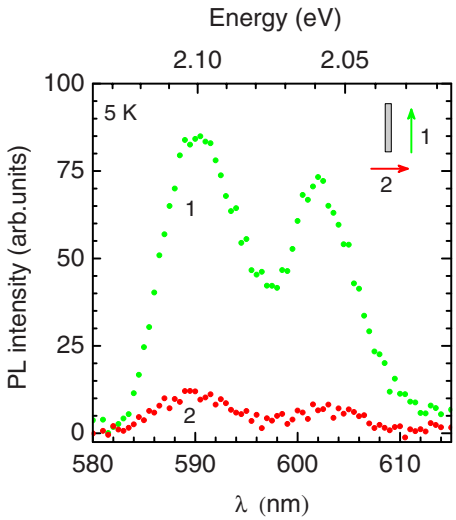

FIG. 4. (Color online) The low temperature polarization-dependent PL spectra of the InAs/AlAs QW taken from the sample edge. Arrows indicate the directions of the electric field vector for the two spectra.

thin GaAs/AlAs QW with a GaAs layer thickness of 2 ML that produced type-II band alignment, (ii) a 100 nm layer of AlAs without any QW formed inside, and (iii) a structure with InAs quantum dots (QDs) formed in an AlAs matrix[33] whose InAs wetting layer represents a QW similar to those described above but has a thickness of 1.8 ML. Sample (i) was grown in a Riber Compact system at T_S=600 °C. The PL excitation was accomplished above the direct band gap of the AlAs matrix. Steady-state PL was excited by a He-Cd laser ($\hbar\omega$=3.81 eV) with a power density in the range of 0.02–25 W cm^{-2}. Transient PL was excited by a pulsed N_2 laser ($\hbar\omega$=3.68 eV) with a pulse duration of 7 ns and a peak power density of 150 kW cm^{-2} or 1 mJ cm^{-2} density of the pulse energy. Stationary and transient PLs were analyzed by a 0.6 m double grating monochromator and detected with a cooled photomultiplier tube with an S-20 photocathode. The PL signal was recorded using a photon counting system for stationary PL and a time-correlated photon counting system in transient PL mode. The degree of linear polarization of QW PL was measured in the edge-emission geometry perpendicular to the growth direction. The laser light was incident normal to the plane of the QW layer, the sample being excited is close to the edge to minimize self-absorption. The polarization degree was analyzed by a polarizer placed in front of the cryostat window. A quartz depolarizer wedge was placed in front of the entrance slit of the monochromator to eliminate spurious polarization effects arising from the grating.

IV. EXPERIMENTAL RESULTS

A. Photoluminescence of InAs/AlAs quantum well

The low temperature PL spectra of the 1.4 ML QW sample and a comparison single AlAs layer are shown in Fig. 3. Two intense PL lines: high energy at 2.102 eV and low energy at 2.060 eV, with full widths at half maximum (FWHMs) of 36 and 22 meV, respectively, dominate in the spectrum of the QW. The lines are Gaussian like with slightly extended low-energy tails. A weak feature around 2.010 eV is also seen. The spectra of the samples with different well widths demonstrate the same bands and low-energy feature that are shifted as a whole, while their relative positions remain constant. In the spectrum of the AlAs layer sample, we observe only a weak broad line at an energy of 2.1 eV connected with the donor-acceptor recombination in AlAs.[34] The intensity of this line is by 3 orders of magnitude smaller than that of the QW sample. The low PL intensity in the AlAs layer is quite natural since, due to the small probability of radiative recombination in an indirect band-gap material, the photoexcited electrons and holes mostly transfer to the surrounding GaAs rather than recombine in this thin layer. The intense PL of the thin InAs QW evidences that the high efficiency of carrier capture by this layer is similar to the case of thin InAs/GaAs QWs.[3,7]

B. Identification of the optical transitions

The PL spectra of thin InAs/AlAs QWs always contain two lines in contrast to the spectra of thin InAs/GaAs or InAs/InP QWs, which display a single excitonic line only.[2–4,7–9] In this section, we will demonstrate that these two PL lines are due to an excitonic transition accompanied by phonon replicas, while other alternative explanations such as transitions involving heavy- and light-hole states in the QW or transitions in regions of the QW with different widths can be rejected.

In order to clarify whether the two PL lines are related to transitions involving heavy and lights holes, we measured linearly polarized PL taken from the edge of the sample. The results are depicted in Fig. 4. One can see that both lines are strongly polarized along the plane of the QW. The polarization of the PL is not complete, though. Such a feature of the polarization spectra can be caused by two reasons: the light-heavy holes mixing[5] or the contribution of unpolarized PL emitted approximately perpendicular to the line of sight and then directed toward the observer by reflections at the sample's surfaces.[4] However, in any case, the high degree of PL

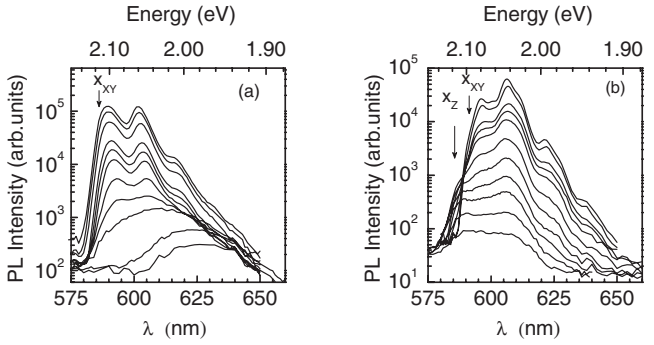

FIG. 5. The spectra of the (a) InAs/AlAs and (b) GaAs/AlAs QWs as a function of temperature, from top to bottom: (a) 5, 10, 15, 20, 25, 30, 40, 50, 60, 90, and 100 K; (b) 5, 10, 20, 25, 30, 40, 50, 60, 70, 85, and 100 K.

polarization along the plane of the QW evidences the heavy-hole character for both transitions.[4]

In order to clarify whether the PL lines are attributed to the well width fluctuations, we studied the PL temperature dependence. The spectra are depicted in Fig. 5(a). One can see that as temperature is increased, both QW related lines simultaneously drop in intensity, and subsequently, disappear under a broad PL band[35] at temperatures above 50 K. The absence of any significant change in relative intensity of the lines clearly evidences that the PL lines are not related to fluctuations of the well width, which should cause an increase in the intensity of the high-energy line.[36–38]

An interesting feature of the InAs/AlAs QW spectra is that the parameters of the PL lines are closely connected together. The relative intensity, linewidth, and energy splitting of the two lines remain similar with changes in temperature and concentration of nonequilibrium carriers (the latter will be demonstrated in Sec. IV C). These observations suggest that the lines correspond to the no-phonon line of an excitonic transition and its phonon replica, or two phonon replicas. However, the splitting of these lines is quite different from any phonon energy in InAs or AlAs.[25] We assume that this is a result of an overlap of a no-phonon (NP) line and several of its replicas related to phonons belonging to InAs and AlAs, all broadened due to the roughness of the QW interface. Since the lowest state of the conduction band of the AlAs matrix has the X_{XY} symmetry,[39] it is reasonable to expect, similar to a type-II band alignment X_{XY} GaAs/AlAs QW, that these phonon replicas are related to (i) longitudinal optical (LO) phonons of InAs ($\hbar\Omega_{LO}^{\mathrm{InAs}}$) =25 meV), (ii) transverse acoustical (TA) phonons of AlAs ($\hbar\Omega_{TA}^{\mathrm{AlAs}}$=12 meV) at point X of the Brillouin zone, and (iii) point X LO phonons of AlAs ($\hbar\Omega_{LO}^{\mathrm{AlnAs}}$=48 meV).[25] Note that the replicas related to the AlAs phonons can be present in a spectrum of a QW not only of type II but also of type-I band alignment. Indeed, in a thin abrupt QW, the carrier wave function extends to the matrix that facilitates interaction with AlAs phonons, while a diffused QW manifests itself as a layer of InAlAs alloy with a high concentration of AlAs. As it is clearly seen in Fig. 3, the FWHM of even the narrowest PL line is at least twice the AlAs TA-phonon energy and is practically the same as the InAs LO-phonon energy; therefore, PL lines of these replicas cannot be resolved in the spectra of InAs/AlAs QWs.

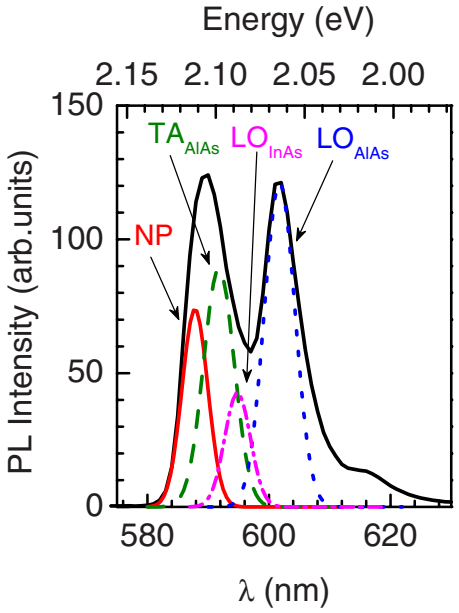

FIG. 6. (Color online) Deconvolution of the PL spectrum of the 1.4 ML InAs/AlAs QW.

Fitting the spectrum with the lines of phonon replicas listed above confirms the assumption on the phonon-related nature of the PL lines. Figure 6 shows the results of fitting of the spectrum with a sum of four Gaussian lines corresponding to the no-phonon transition and its TA_{AlAs}, LO_{AlAs}, and LO_{InAs} replicas. The best agreement between the experimental and fitted spectra has been achieved for the no-phonon transition energy of 2.109 eV. A small deviation of the low-energy side in the experimental spectrum is connected with two-phonon lines, which were not taken into account in the fitting. Note that in the framework of the proposed interpretation, the weak line at 2.010 eV finds a natural explanation as a two-LO_{AlAs}-phonon transition.

C. Determination of the quantum well band lineup

The identification of the lines in the PL spectra of thin InAs/AlAs QWs as phonon replicas shows only that electrons reside in indirect X_{XY} states, but does not help us to discriminate between the types of alignment of conduction bands in the studied structures. In order to determine the band lineup of the InAs/AlAs QWs, we studied the energy position of the PL lines ($\hbar\omega_{max}$) as a function of the concentration (n) of nonequilibrium carriers.

The $\hbar\omega_{max}(n)$ dependence in structures with type-II band alignment was analyzed in Ref. 5. It has been shown that the shift in the line position is proportional to the cubic root of the excitation power density at densities as small as 0.05 W cm^{-2} (see Refs. 5 and 40). In structures with type-I band alignment, $\hbar\omega_{max}$ is determined by the product of the densities of states and functions of band occupancies for electrons and holes.[41] In this case, $\hbar\omega_{max}$ does not depend on the excitation power density until the carrier quasi-Fermi-

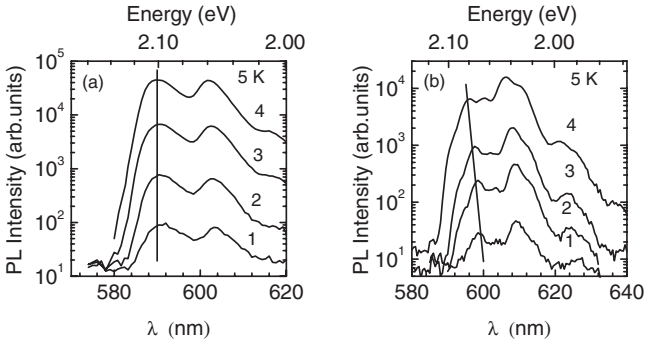

FIG. 7. The low temperature PL spectra of the (a) InAs/AlAs and (b) GaAs/AlAs QWs as a function of excitation power density (W cm^{-2}): (a) 1, 0.04; 2, 0.35; 3, 3.2; 4, 25; (b) 1, 0.02; 2, 0.14; 3, 1.3; 4, 12.

levels enter the respective bands and band filling begins. A further increase in the excitation density results in a blueshift of the line.[41]

The cw PL spectra as a function of excitation power density are depicted in Fig. 7(a). For comparison, the spectra of the type-II GaAs/AlAs QW taken with similar excitation densities are presented in Fig. 7(b). One can see that the increase of the excitation power density by almost 3 orders of magnitude practically does not lead to any shift of the lines in the InAs/AlAs QW, while in the spectra of the GaAs/AlAs QW, the lines display a 7 meV shift in the same power range. The dependencies of the line shift on excitation density for the two structures are shown in Fig. 8. It is seen that in the type-II GaAs/AlAs QW the shift is proportional to the cubic root of the excitation power density, in agreement with Refs. 5 and 40.

The transient PL spectra of the InAs/AlAs and GaAs/AlAs QWs with a nitrogen laser excitation are depicted in Fig. 9. In the InAs/AlAs QW, in spite of the high peak excitation power density of 150 kW cm^{-2}, only a small redshift (8 meV) of the lines connected with filling of the bands with nonequilibrium carriers takes place during the

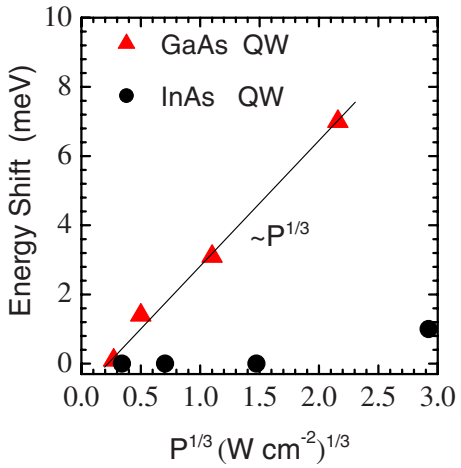

FIG. 8. (Color online) The shift of the PL lines of the InAs/AlAs and type-II GaAs/AlAs QWs as a function of excitation power density P.

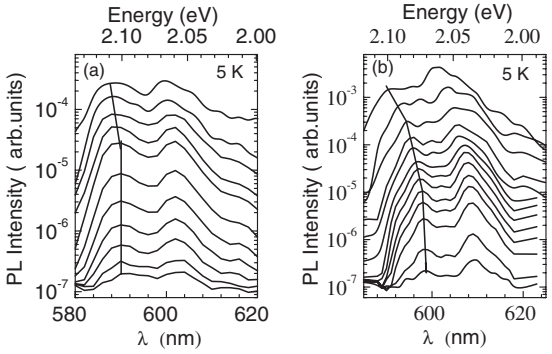

FIG. 9. Transient PL spectra of the (a) InAs/AlAs and (b) GaAs/AlAs QWs. The delays after the excitation pulse, from top to bottom: (a) 0.25, 2, 20, 50, 150, 250, 350, 450, 550, 650, and 750 ms; (b) 0.25, 0.6, 2, 10, 40, 100, 200, 400, 700, 1000, 1500, 2600, and 3600 ms.

initial stage of decay, when the PL intensity decreases several times.[41] On the other hand, the PL lines of the GaAs/AlAs QW demonstrate a continuous redshift during the decay that reaches 30 meV some 3 ms after the excitation pulse. Therefore, the absence of the shift of the lines with variation in the concentration of nonequilibrium carriers at moderate excitation densities allows us to identify the spatial band alignment of the InAs/AlAs QW as type I.

It is interesting that the InAs/AlAs and GaAs/AlAs QWs display not only different line shifts in the transient PL spectra but also different laws of decay, as illustrated in Fig. 10. The InAs/AlAs QW demonstrates a virtually exponential PL decay with a lifetime of 110 μs (fit curve 1), while the GaAs/AlAs QW displays a nonexponential decay that is almost an order of magnitude longer (see inset; note the use of double logarithmic plot). In order to demonstrate that this difference supports the conclusion on type-I band alignment in the InAs/AlAs QW, we present below an analysis of the PL decay law.

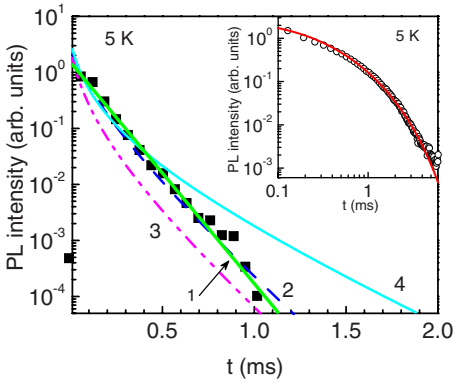

FIG. 10. (Color online) The kinetics of the integrated PL of the InAs/AlAs QW (empty squares). Lines are decay curves calculated according to Eq. (7) with decay rates (s^{-1}): 1, $w_0=9\times10^3$, $w_r=0$ (pure exponential); 2, $w_0=6\times10^3$, $w_r=4\times10^3$; 3, $w_0=6\times10^3$, $w_r=8\times10^3$; and 4, $w_0=3\times10^3$, $w_r=8\times10^3$. Inset: Type-II GaAs/AlAs QW PL decay (empty circles) and calculated decay curve for $w_0=6\times10^2$ s^{-1} and $w_r=1.5\times10^3$ s^{-1}.

It is known that the PL decay of X_{XY} indirect band-gap QWs of both types of band alignment[42–44] and with any structure of the heterointerface[42,45] (abrupt or diffused) can be described with the following relationship for the recombination rate I_{PL}:

$$I_{PL}(t) \propto \exp(-w_0 t)(1+2w_r t)^{-3/2}, \quad (7)$$

where t is time, w_r is the decay rate connected with stochastic processes of scattering of electronic momenta by short-range potential scatterers related to any imperfection of atomic structure, and w_0 is the decay rate resulting from other processes not related to stochastic scattering, including all recombination channels: phonon-related radiative and extrinsic nonradiative recombinations. The decay curves calculated in accordance with Eq. (7) for different values of w_0 and w_r are depicted in Fig. 10. In the case of the GaAs/AlAs QW, the best approximation of the experimental decay was obtained with $w_0=6\times10^2$ s^{-1} and $w_r=1.5\times10^3$ s^{-1}, which are similar to the values obtained earlier for X_{XY} GaAs/AlAs short-period superlattices.[42,43] In the InAs/AlAs QW, the calculated decay curve satisfactorily fits the experimental data, with the parameters w_0 and w_r lying in the ranges $w_0=(6-9)\times10^3$ s^{-1} and $w_r=(0-4)\times10^3$ s^{-1} (curves 1 and 2 in the figure). With w_r greater than 4×10^3 s^{-1}, no fit could be obtained for any value of w_0 (see curves 3 and 4 as an example).[46]

The most interesting result is the increase of w_0 in the InAs/AlAs QW by an order of magnitude in comparison with the GaAs/AlAs QW. We interpret this strong increase in w_0 as a result of type-I band alignment in InAs/AlAs QWs. Indeed, in the case of type-I alignment QWs, the overlap of the electron and hole wave functions takes place not only at the heterointerface but also everywhere inside the QW. This results in an increase of the probability of radiative recombination of excitons accompanied by phonon emission that is responsible for the w_0 value. It is also possible that the increase in w_0 is related to the increase in nonradiative recombination rate.[45,47] Since the intensities of cw PL of both QWs measured under the same experimental conditions are similar, the nonradiative losses in the InAs/AlAs QW are compensated by an increase in the rate of carrier capture by the QW. It is known that the rate of carrier capture in a QW of type I is much larger than in a type-II QW.[48] Thus, the increase in w_0 due to the discussed reasons also indicates the type-I band alignment in the thin InAs/AlAs QW.

A further argument in favor of type-I alignment in the InAs/AlAs QW is given by a comparison of the temperature dependencies of the PL spectra seen in the InAs/AlAs and GaAs/AlAs QWs [Figs. 5(a) and 5(b)]. One can see that an increase in temperature leads to the appearance of a high-energy line in the spectra of type-II GaAs/AlAs QW. This line is related to the recombination of X_Z excitons due to the filling of X_Z states of the AlAs conduction band by electrons at high temperatures.[49] At the same time, this line does not appear in the spectra of InAs/AlAs QWs.

D. Identification of the atomic structure of an InAs/AlAs quantum well

The PL spectrum deconvolution presented in Fig. 6 reveals a domination of the AlAs-related phonon replicas in the spectrum of type-I alignment InAs/AlAs QW. This is an argument in favor of a diffused structure of the QW. Indeed, in such a case, the QW manifests itself as a layer of an InAlAs alloy with a high concentration of AlAs; therefore, a domination of AlAs-related phonon replicas in the spectrum is quite natural. In this section, in order to find additional arguments in favor or against the suggestion of the diffused atomic structure of the InAs/AlAs QW, we analyze the energy position of the QW PL lines as a function of the QW width.

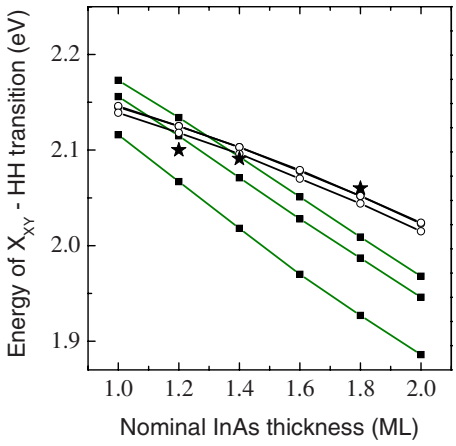

FIG. 11. (Color online) Calculated energy of the electron–heavy hole transition as a function of the nominal QW thickness. Full squares, abrupt QW; empty circles, diffused QW. The VBO values, from top to bottom in each set (eV): 0.8, 0.5, and 0.3. The experimental data (energy position of the high-energy PL line) are depicted with stars.

Figure 11 demonstrates that the InAs/AlAs QWs with a nominal thicknesses of 1.2 and 1.4 ML and the 1.8 ML thick wetting layer of the structure with InAs/AlAs QDs have close energy positions of the high-energy PL line (the data on the QD sample were taken from our recent work[33]): as the well thickness is varied 1.5 times, the position of the line changes by 40 meV only. The calculated energies of the electron to heavy hole transition as a function of the nominal QW thickness in abrupt and diffused QWs are shown in Fig. 11 for several VBO values.[50] The calculation was performed in the framework of the envelope function model.[51] One can see that the energy of the optical transitions calculated for diffused QWs is very close to the experimental data (stars), while that in the abrupt QW depends considerably strongly on the QW width. Besides, 1 min annealing of the QD sample at 850 °C had shown that the PL lines of the wetting layer are blueshifted by only 10 meV, whereas the QD line exhibits a blueshift of more than 200 meV due to the InAs-AlAs interdiffusion.[33] The small blueshift of the wetting layer's QW line evidences that the wetting layer is initially a diffused QW, and the additional interdiffusion induced by the annealing only slightly changes its shallow potential profile.[33]

Therefore, we conclude that thin InAs/AlAs QWs are diffused QWs with type-I band alignment and that the lowest electron state belongs to the X_{XY} minimum of the conduction band.

V. CONCLUSION

The energy spectrum and structure of thin InAs QWs in an AlAs matrix have been investigated. We determined that the QWs are diffused InAlAs layers like those observed recently by Offermans *et al.*,[13] and have type-I band alignment. The calculation of the QW energy structure and the shape of the PL spectrum demonstrate that the lowest state of the QW conduction band belongs to the X_{XY} indirect minimum. The intense PL of the QWs demonstrates the high efficiency of carrier capture by a thin InAs layer with respect to bulk AlAs material.

ACKNOWLEDGMENT

The authors wish to thank L. S. Braginsky for valuable discussions. The authors acknowledge the financial support of the Russian Foundation for Basic Research (Grant No. 07-02-00134).

*timur@thermo.isp.nsc.ru

[1] N. N. Ledentsov, P. D. Wang, C. M. Sotomayor Torres, A. Y. Egorov, M. V. Maximov, V. M. Ustinov, A. E. Zhukov, and P. S. Kop'ev, Phys. Rev. B **50**, 12171 (1994).
[2] M. I. Alonso, M. Ilg, and K. H. Ploog, Phys. Rev. B **50**, 1628 (1994).
[3] O. Brandt, L. Tapfer, R. Cingolani, K. Ploog, M. Hohenstein, and F. Phillipp, Phys. Rev. B **41**, 12599 (1990).
[4] O. Brandt, H. Lage, and K. Ploog, Phys. Rev. B **45**, 4217 (1992).
[5] N. N. Ledentsov *et al.*, Phys. Rev. B **52**, 14058 (1995).
[6] G. H. Li, A. R. Goni, C. Abraham, K. Syassen, P. V. Santos, A. Cantarero, O. Brandt, and K. Ploog, Phys. Rev. B **50**, 1575 (1994).
[7] J. Brübach, A. Y. Silov, J. E. M. Haverkort, W. van der Vleuten, and J. H. Wolter, Phys. Rev. B **61**, 16833 (2000).
[8] J. Arriaga, G. Armelles, M. C. Munoz, J. M. Rodriguez, P. Castrillo, M. Recio, V. R. Velasco, F. Briones, and F. Garcia-Moliner, Phys. Rev. B **43**, 2050 (1991).
[9] P. Paki, R. Leonelli, L. Isnard, and R. A. Masut, Appl. Phys. Lett. **74**, 1445 (1999).
[10] N. Shtinkov, P. Desjardins, and R. A. Masut, Phys. Rev. B **66**, 195303 (2002).
[11] J. Urayama, T. B. Norris, H. Jiang, J. Singh, and P. Bhattacharya, Appl. Phys. Lett. **80**, 2162 (2000).
[12] W. Yang, R. R. Lowe-Webb, H. Lee, and P. C. Sercel, Phys. Rev. B **56**, 13314 (1997).
[13] P. Offermans, P. M. Koenraad, R. Notzel, J. H. Wolter, and K. Pierz, Appl. Phys. Lett. **87**, 111903 (2005).
[14] G. Ghislotti, E. Riedo, D. Ielmini, and M. Martinelli, Appl. Phys. Lett. **75**, 3626 (1999).
[15] T. Asano, S. Noda, T. Abe, and A. Sasaki, J. Appl. Phys. **82**, 3385 (1997).
[16] J. M. Jancu, V. Pellegrini, R. Colombelli, F. Beltram, B. Mueller, L. Sorba, and A. Franciosi, Appl. Phys. Lett. **73**, 2621 (1998).
[17] C. G. Van de Walle, Phys. Rev. B **39**, 1871 (1989).
[18] A. Stroppa and M. Peressi, Phys. Rev. B **71**, 205303 (2005).
[19] S. H. Wei and A. Zunger, Phys. Rev. B **60**, 5404 (1999).
[20] M. C. Muñoz and G. Armelles, Phys. Rev. B **48**, 2839 (1993).
[21] I. Vurgaftman, J. R. Meyer, and L. R. Ram-Mohan, J. Appl. Phys. **89**, 5815 (2001).
[22] B. K. Ridley, J. Appl. Phys. **48**, 754 (1977).
[23] *Semiconductor Optics and Transport Phenomena*, edited by W. Schafer and M. Wegener (Springer, Berlin, 2002).
[24] T. B. Boykin, Phys. Rev. B **56**, 9613 (1997).
[25] *Numeral Data and Functional Relationships in Science and Technology*, edited by O. Madelung, H. Weiss, and M. Schulz, Landolt-Börnstein, New Series, Group III (Crystal and Solid State Physics), Vol. 17 (Springer, Heidelberg, 1982).
[26] S. Adachi, J. Appl. Phys. **61**, 4869 (1987).
[27] *Handbook Series on Semiconductor Parameters*, edited by M. Levinshtein, S. Rumyantsev, and M. Shur (World Scientific, Singapore, 1996), Vol. 1; (World Scientific, Singapore, 1996), Vol. 2.
[28] S. H. Wei and A. Zunger, Appl. Phys. Lett. **72**, 2011 (1998).
[29] S.-P. Li, R.-Z. Wang, Y.-M. Zheng, S.-H. Cai, and G.-M. He, J. Phys.: Condens. Matter **12**, 7759 (2000).
[30] C. Ohler, A. Förster, J. Moers, C. Daniels, and H. Lüth, J. Phys. D **30**, 1436 (1997).
[31] S. H. Ke, R. Z. Wang, and M. C. Huang, Phys. Rev. B **49**, 10495 (1994).
[32] K. Muraki, S. Fukatsu, Y. Shiraki, and R. Ito, Appl. Phys. Lett. **61**, 557 (1992).
[33] T. S. Shamirzaev, A. K. Kalagin, A. I. Toropov, and K. S. Zhuravlev, Phys. Status Solidi C **3**, 3932 (2006).
[34] L. Pavesi and M. Guzzi, J. Appl. Phys. **75**, 4779 (1994).
[35] Previously, we had observed a similar broad band in type-II alignment GaAs/AlAs short perdiocal superlattices, and had attributed it to donor-to-acceptor transitions [see K. S. Zhuravlev, D. A. Petrakov, A. M. Gilinsky, T. S. Shamirzaev, V. V. Preobrazhenskii, B. R. Semyagin, and M. A. Putyato, Superlattices Microstruct. **28**, 105 (2000)]. The broad band in the InAs/AlAs QWs demonstrates the same temperature dependencies of the position and intensity as well as transient PL kinetics as those of the band in type-II GaAs/AlAs superlattices. Therefore, we attribute this band to type-II donor-to-acceptor transitions, with donors localized in the AlAs layers and acceptors localized in the InAs layer.
[36] K. K. Bajaj, Mater. Sci. Eng., B **79**, 203 (2001).
[37] U. Jahn, S. H. Kwok, M. Ramsteiner, R. Hey, H. T. Grahn, and E. Runge, Phys. Rev. B **54**, 2733 (1996).
[38] F. Martelli, A. Polimeni, A. Patane, M. Capizzi, P. Borri, M. Gurioli, M. Colocci, A. Bosacchi, and S. Franchi, Phys. Rev. B **53**, 7421 (1996).
[39] The X conduction band minima of an AlAs layer grown on a GaAs substrate are split due to the difference in the lattice parameters of GaAs and AlAs, X_{XY} subband being the lowest in energy.
[40] F. Hatami *et al.*, Appl. Phys. Lett. **67**, 656 (1995).
[41] S. K. Brieley, J. Appl. Phys. **74**, 2760 (1993).
[42] F. Minami, K. Hirata, K. Era, T. Yao, and Y. Masumoto, Phys. Rev. B **36**, 2875 (1987).
[43] L. S. Braginsky, M. Y. Zaharov, A. M. Gilinsky, V. V. Preobrazhenskii, M. A. Putyato, and K. S. Zhuravlev, Phys. Rev. B

63, 195305 (2001).
[44] D. S. Citrin, Phys. Rev. B **51**, 2608 (1995).
[45] M. V. Klein, M. D. Sturge, and E. Cohen, Phys. Rev. B **25**, 4331 (1982).
[46] The short-range potential responsible for the w_r rate causes no-phonon radiative recombination of excitons (Refs. 43 and 45). A comparison of the cw PL spectra of the InAs/AlAs and GaAs/AlAs QWs demonstrates that the relative intensity of the no-phonon line is greater by an order of magnitude in the InAs/AlAs QW. Therefore, the density of the short-range potential fluctuations and w_r increase when going from the GaAs/AlAs to InAs/AlAs QW. In abrupt QWs, this increase in w_r can result from an increase in the density of scatterers caused by steplike roughness of flat heterointerfaces. In diffused QWs, this increase in w_r can be caused by the compositional disorder (Ref. 45).
[47] I. N. Krivorotov, T. Chang, G. D. Gilliland, L. P. Fu, K. K. Bajaj, and D. J. Wolford, Phys. Rev. B **58**, 10687 (1998).
[48] B. K. Ridley, Phys. Rev. B **50**, 1717 (1994).
[49] P. Dawson, C. T. Foxon, and H. W. van Kesteren, Semicond. Sci. Technol. **5**, 54 (1990).
[50] In order to calculate the energy of the lowest electron state, we take E_X=1.433 eV that results in a type-I alignment for both the abrupt and diffused QWs. A variation in E_X shifts the position of the electron state, but does not change the main result of the calculation: the strong dependence of the transition energy on the thickness for an abrupt QW.
[51] Although the use of the envelope function model for calculations in QWs of just a few monolayers in thickness is not perfectly justified, this model gives good agreement with PL and PL excitation data (Ref. 3), and was therefore applied here.